

Strait of Messina

based on the article *Internal Waves in the Strait of Messina Studied by a Numerical Model and Synthetic Aperture Radar Images from the ERS 1/2 Satellites* by P. Brandt, A. Rubino, W. Alpers, and J. O. Backhaus [1997] with permission of the authors

Overview

The Strait of Messina separates the Italian Peninsula from the Italian island of Sicily and connects the Tyrrhenian Sea in the north with the Ionian Sea in the south (Figure 1). The strait is a narrow channel, whose smallest cross-sectional area is 0.3 km² in the sill region. There, the mean water depth is 80 m. While in the southern part of the strait the water depth increases rapidly (a depth of 800 m is encountered approximately 15 km south of the sill), in the northern part it increases more gently (a depth of 400 m is encountered approximately 15 km north of the sill). Throughout the year, two different water masses are present in the Strait of Messina: the Tyrrhenian surface water (TSW) and the colder and saltier Levantine Intermediate Water (LIW).

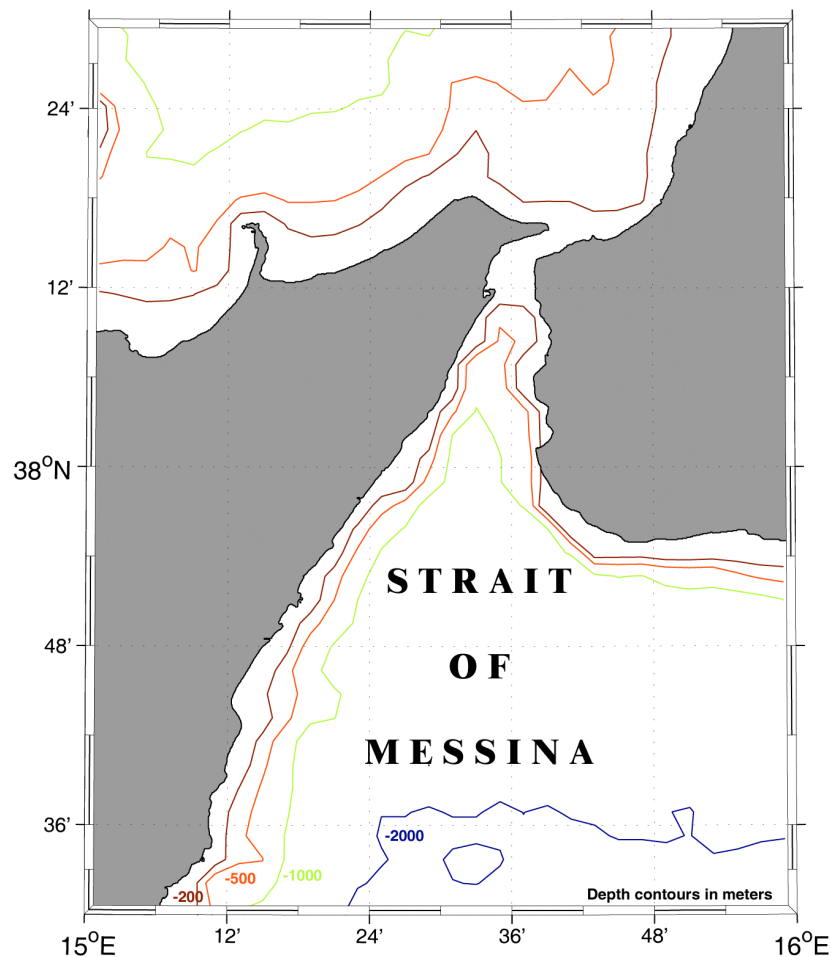


Figure 1. Bathymetry of the Strait of Messina and surrounding region.

In the vicinity of the Strait of Messina these water masses are separated at a depth of about 150 m [Vercelli 1925]. During most of the year, a seasonal thermocline is also present in the strait. Across this interface the difference in the water density is, in general, much larger than across the interface between the LIW and TSW. Although tidal displacements are very small in the Mediterranean Sea (of the order of 10 cm), large gradients of tidal displacements are present in the Strait of Messina, because the predominantly semidiurnal tides north and south of the strait are approximately in phase opposition. Due to the phase opposition of the tides and due to topographic constrictions, the current velocities in the Strait of Messina can attain values as high as 3.0 m/s_i in the sill region. There is also a weak mean exchange flow through the strait; while the mean flow of the surface layer is directed toward the Ionian Sea with a velocity of approximately 0.10 m/s, the mean flow in the lower layer is directed toward the Tyrrhenian Sea with a velocity of approximately 0.13 m/s. This mean exchange can strongly fluctuate, depending on wind and air pressure changes. Velocities of the mean flow up to 0.5 m/s may be present at the sill [Vercelli 1925; Defant 1940, 1961]. For more detailed information on the hydrodynamics of the Strait of Messina the reader is referred to the review paper of Bignami and Salusti [1990].

Observations

There has been considerable scientific study of internal waves in the Strait of Messina through both in situ and satellite observations. The first satellite observations of internal solitary waves were made by SEASAT on 15 September 1978. The three rings visible on the SEASAT SAR image in the Tyrrhenian Sea north of the strait were interpreted as sea surface manifestations of a train of internal solitary waves propagating northward [Alpers and Salusti 1983]. In the following years, oceanographic campaigns were carried out to measure internal solitary waves north and south of the strait. In November 1980 two northward propagating internal wave trains were detected in temperature data records at a position 25 km north of the strait. The time lag between the time of arrival of the two wave trains at this position was 11 h 30 min, which agrees well to the time interval of 11 h 22 min between the two successive tidal flow reversals at the strait's sill, identified as the release times of the observed internal bores from the sill [Alpers and Salusti 1983; Griffa et al. 1986]. During an oceanographic cruise from May to June 1982, Sapia and Salusti [1987] detected in temperature data records two trains of internal solitary waves north of the strait. During this cruise oceanographic measurements were also carried out south of the strait, which revealed the existence of large amplitude isolated signals in the temperature data records south of the sill and as far as to the coast of Syracuse. By using temperature sensors and a KODEN fish finder, Di Sarra et al. [1987] observed a 100-m deep depression of the interface between the water masses in the zone immediately south of the sill. The first observation of a well-developed internal wave train south of the sill was made by the LANDSAT thematic mapper (TM) [Artale et al. 1990]. In October 1987 Nicolò and Salusti [1991] also observed in temperature records three large amplitude internal wave trains south of the sill.

Beginning in 1991, the ERS-1/2 satellites have acquired SAR imagery over the Strait of Messina and the adjacent sea areas. In this investigation, 160 satellite overflights over the sea areas north and south of the sill between 1991 and 1995 have been examined. Sea surface manifestations of internal waves could be delineated in imagery from 77 of the 160 overflights. It should be noted that due to the different orbits flown by the ERS-1/2 satellites, so more SAR

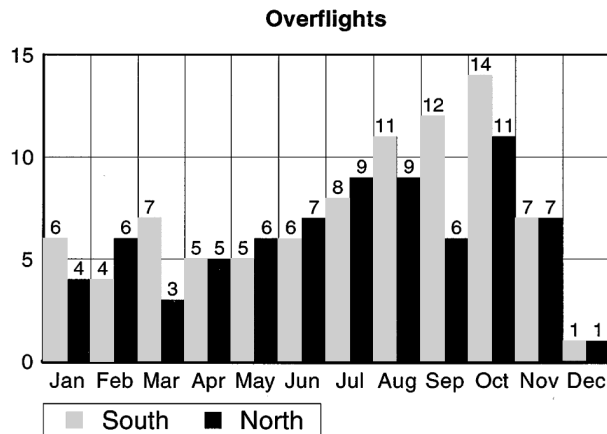


Figure 2. Number of ERS-1/2 overflights per month over the Strait of Messina and adjacent sea areas between 1 December 1991 and 31 December 1995. Gray bars denote overflights during which SAR images over the region south of the sill were acquired, black bars denote overflights during which SAR images over the region north of the sill were acquired.

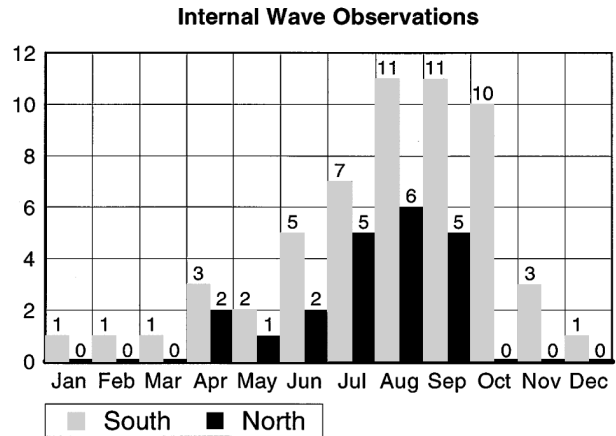


Figure 3. Number of internal wave observations per month made on the ERS-1/2 SAR images listed in Figure 2. Gray bars denote internal wave observations south of the sill, black bars internal wave observations north of the sill.

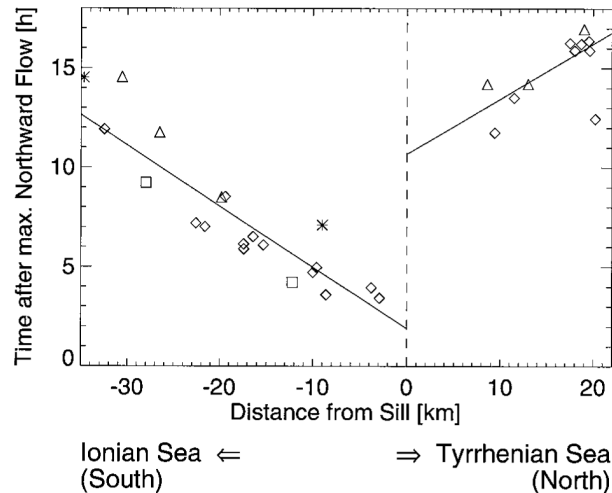


Figure 4. Space–time diagram showing the propagation of the front of northward and southward propagating internal wave trains in the Strait of Messina as inferred from ERS-1/2 SAR images. Diamonds refer to observations made between July and September, triangles to observations made between April and June, squares to observations made between October and December, and stars to observations made between January and March. The lines are least square fits that yield for the front of northward and southward propagating internal waves trains the propagation speeds 1.00 m s^{-1} and 0.91 m s^{-1} , respectively.

images were acquired over the Strait of Messina in the period from April to November than in the period from December to March (see Figure 2). The analysis of the available ERS-1/2 SAR images shows that sea surface manifestations of internal waves are observed more frequently during periods where a strong seasonal thermocline is known to be present, that is, during summer. Furthermore, sea surface manifestations of southward propagating internal waves can be delineated on ERS-1/2 SAR images more frequently than those of northward propagating ones (Figure 3). In general, sea surface manifestations of southward propagating internal waves are stronger than those of northward propagating ones. Figure 4 shows a time versus distance diagram delineating the propagation of internal bores north and south of the sill as inferred from the analyzed ERS-1/2 SAR images. In this figure, the distance between the fronts of internal,

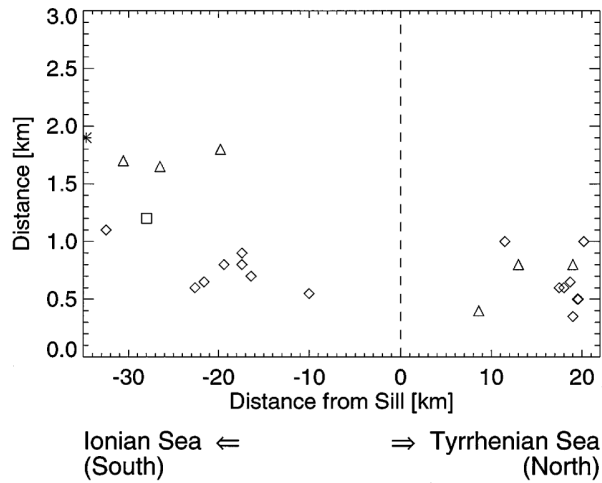


Figure 5. Spatial separation between the first two internal solitary waves of northward and southward propagating wave trains as a function of distance from sill as inferred from ERS-1/2 SAR images. Diamonds refer to observations made between July and September, triangles to observations made between April and June, the square refers to an observation made between October and December, and the star to an observation made between January and March.

wave trains and the sill referenced to the time of maximum northward tidal flow at Punta Pezzo, is depicted. This distance is measured along a mean path of the center of the wave fronts, which is inferred from the available ERS-1/2 SAR images. The lines are least square fits that yield for the northward propagating waves an average propagation speed of 1.00 m/s and for the southward propagating waves an average propagation speed of 0.91 m/s. From this figure, the time of release of internal bores from the sill can be estimated: Southward propagating internal bores are released from the sill between 1 and 5 hours after maximum northward tidal flow at Punta Pezzo, northward propagating internal bores between 2 and 6 hours after maximum southward tidal flow at Punta Pezzo, that is, between 8 and 12 hours after maximum northward tidal flow at Punta Pezzo. Figure 5 shows the spatial separation between the first two internal solitary waves of northward and southward propagating wave trains as a function of the distance from sill as inferred from ERS-1/2 SAR images. This spatial separation ranges from 500 m to 1900 m for southward propagating wave trains, and from 350 m to 1000 m for northward propagating wave trains in the region considered here. Figure 5 shows that, in general, the spatial separation between the first two internal solitary waves of southward propagating wave trains is smaller in the period from July to September than in the period from October to June.

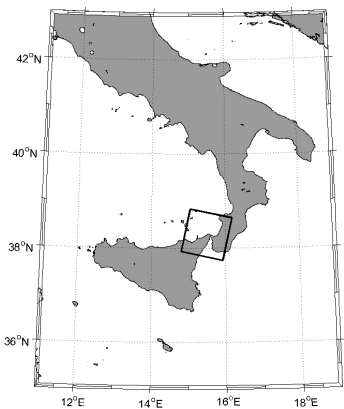
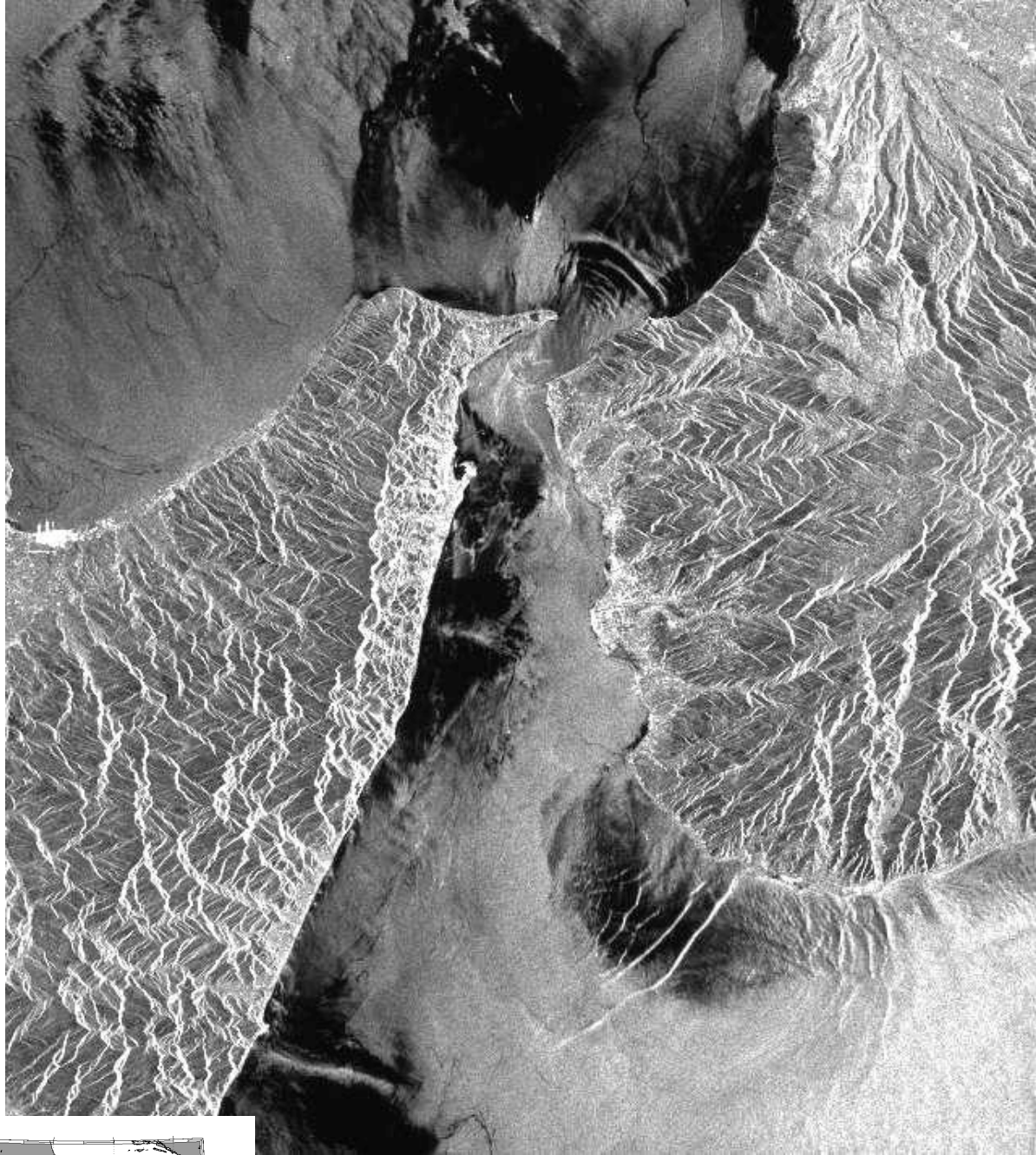


Figure 5. ERS-1 (C-band VV) SAR image of the Strait of Messina acquired on 11 July 1993 at 0941 UTC (orbit 10387, frame 2835). The image shows internal wave signatures radiating out of the strait in both the northern and southern directions. Northwards propagating internal waves are less frequently observed than southward propagating ones. Imaged area is 65 km x 65 km. ©ESA 1993. [From The Tropical and Subtropical Ocean Viewed by ERS SAR <http://www.ifm.uni-hamburg.de/ers-sar/>]

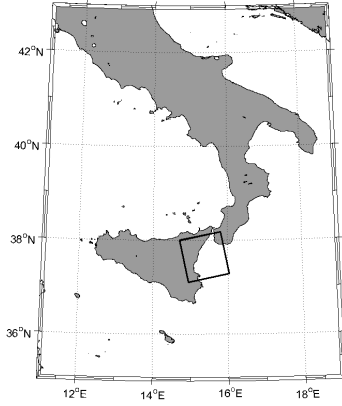


Figure 6. ERS-1 (C-band VV) SAR image of the Strait of Messina acquired on 22 September 1994 at 2115 UTC (orbit 16672, frame 0747). The image shows signatures of three internal wave packets propagating south out of the strait. The signature of the middle is less intense than the leading and trailing packets. Imaged area is 100 km x 100 km. ©ESA 1994. [From The Tropical and Subtropical Ocean Viewed by ERS SAR <http://www.ifm.uni-hamburg.de/ers-sar/>]



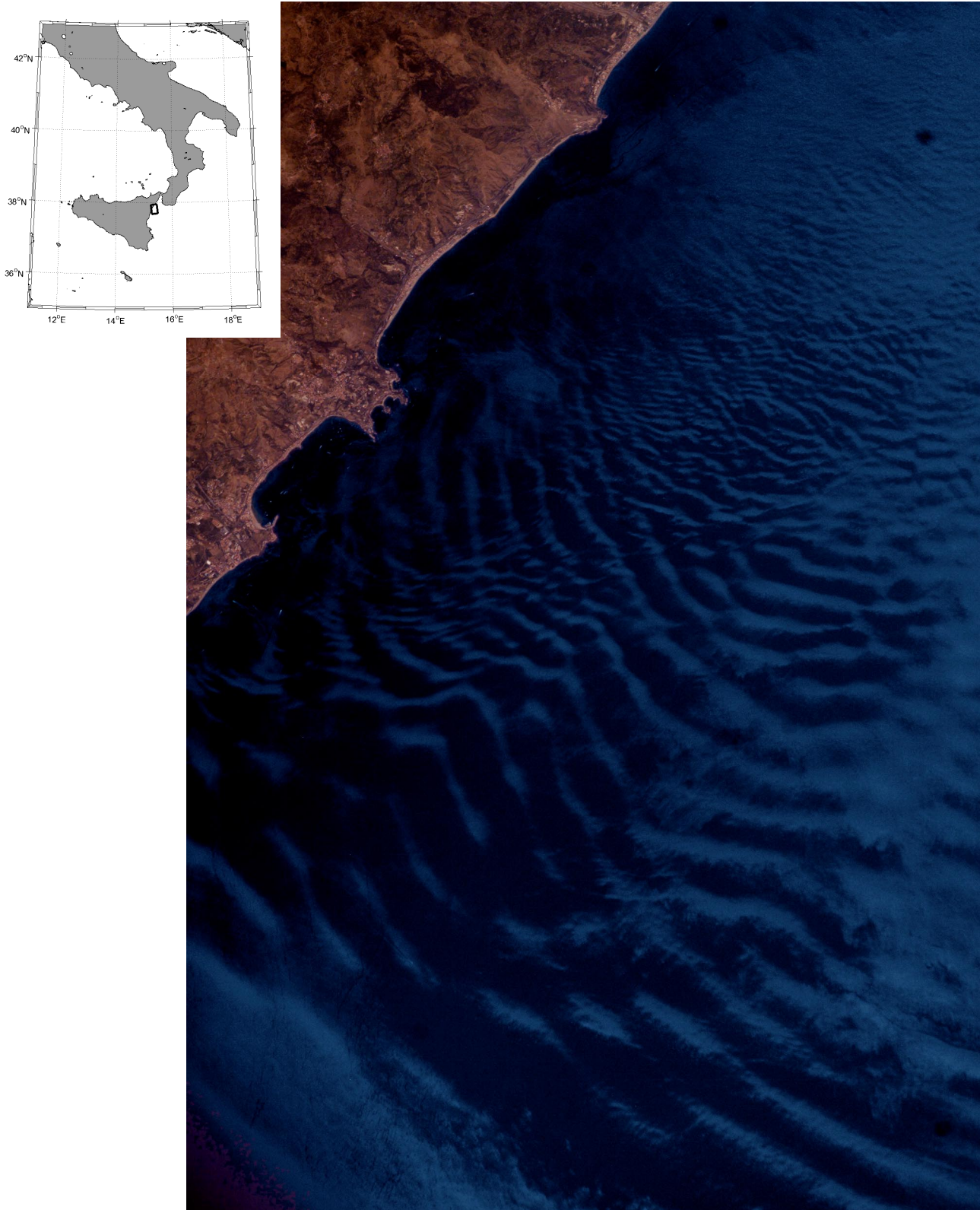


Figure 7. Astronaut photograph (ISS007-E-12283) acquired on 10 August 2003 at 1122 UTC. The image shows an internal wave packet propagating south along the Italian coast. Imaged area is approximately 16 km x 32 km. [Image Courtesy of Earth Sciences and Image Analysis Laboratory, NASA Johnson Space Center (<http://eol.jsc.nasa.gov>)]

References

- Alpers, W., and E. Salusti, 1983: Scylla and Charybdis observed from space. *J. Geophys. Res.*, **88 (C3)**, 1800-1808.
- Artale, V., D. Levi, S. Marullo, and R. Santoleri, 1990: Analysis of nonlinear internal waves observed by Landsat thematic mapper. *J. Geophys. Res.*, **95**, 16 065–16 073.
- Brandt, P., A. Rubino, W. Alpers, and J.O. Backhaus, 1997: Internal waves in the Strait of Messina studied by a numerical model and synthetic aperture radar images from the ERS 1/2 Satellites. *J. Phys. Oceanogr.*, **27 (5)**, 648-663.
- Bignami, F., and E. Salusti, 1990: Tidal currents and transient phenomena in the Strait of Messina: A review. *The Physical Oceanography of Sea Straits*, L. J. Pratt, Ed., Kluwer Academic, 95–124.
- Defant, A., 1940: Scylla und Charybdis und die Gezeitenströmungen in der Strasse von Messina. *Annalen der Hydrographie und Maritimen Meteorologie*, **5**, 145–157.
- Defant, A., 1961: *Physical Oceanography*. Vol. 2. Pergamon, 598 pp.
- Di Sarra, A., A. Pace, and E. Salusti, 1987: Long internal waves and columnar disturbances in the Strait of Messina. *J. Geophys. Res.*, **92**, 6495-6500.
- Griffa, A., S. Marullo, R. Santoleri, and A. Viola, 1986: Note on internal nonlinear tidal waves generated at the Strait of Messina. *Continental Shelf Research*, **6**, 677-687.
- Nicolò, L., and E. Salusti, 1991: Field and satellite observations of large amplitude internal tidal wave trains south of the Strait of Messina, Mediterranean Sea. *Ann. Geophys.*, **9**, 534-539.
- Sapia, A., and E. Salusti, 1987: Observation of nonlinear internal solitary wave trains at the northern and southern mouths of the Strait of Messina. *Deep-Sea Res.*, **34 (7A)**, 1081-1092.
- Smith, W. H. F., and D. T. Sandwell, Global seafloor topography from satellite altimetry and ship depth soundings, *Science*, v. 277, p. 1957-1962, 26 Sept., 1997. http://topex.ucsd.edu/marine_topo/mar_topo.html
- Vercelli, F., 1925: Il regime delle correnti e delle maree nello stretto di Messina. Commissione Internazionale del Mediterraneo, negli Anni 1922 e 1923, 209 pp.

Related Publications

- Alpers, W., P. Brandt, A. Rubino, and J.O. Backhaus, 1996: Recent contributions of remote sensing to the study of internal waves in the Strait of Gibraltar and Messina. *Dynamics of Mediterranean Straits and Channels*. ed. by F. Briand, *CIESM Science Series*, **17 (2)**, 21-40
- Androsov, A.A., N.Ye. Vol'tsinger, B.A. Kagan, and E. Salusti, 1994: Residual tidal circulation in the Strait of Messina. *Phys. Atmos. Ocean*, **29**, 522-531.
- Brandt, P., A. Rubino, D. Quadfasel, W. Alpers, J. Sellschopp, and H.-V. Fiekas, 1999: Evidence for the influence of atlantic-ionian stream fluctuations on the tidally induced internal dynamics in the Strait of Messina. *J. Phys. Oceanogr.*, **29 (5)**, 1071-1080.
- Del Ricco, R., 1982: A numerical model of the vertical circulation of tidal strait and its application to the Messina Strait. *Nuovo Cimento Soc. Ital. Fis.*, **5C**, 21-45.
- Hopkins, T.S., E. Salusti, and D. Settini, 1984: Tidal forcing of the water mass interface in the Strait of Messina. *J. Geophys. Res.*, **89**, 2013-2024.
- Marullo, S., and R. Santoleri, 1986: Fronts and internal currents at the northern mouth of the Strait of Messina. *Nuovo Cimento C.*, **9**, 701-714.